Positioning of objects behind corners using X-band radar

Magnus Gustafsson

Swedish Defence Research Agency, FOI
P.O. Box 1165, SE-58111 Linköping (Sweden)
magnus.gustafsson@foi.se

Abstract

In this paper we present an algorithm for location of stationary objects behind corners using an X-band radar. A street-like scenario is considered. The algorithm relies on the estimation of a reference signal calculated with Geometrical Optics and diffraction theory. By using multipath propagation, we show by means of simulations that it is possible to locate objects behind corners using an X-band radar.

1. Introduction

In urban warfare or for surveillance purposes, having a stand off radar system with the capability of seeing behind corners, in the shadow region, could be of great importance. By using multipath propagation and the diffracted field behind the corners we have showed that a radar system can detect moving objects behind corners when the radar is out of the line-of-sight from the target [1-4]. In these experiments a semi-monostatic single receiver-transmitter radar system was used as a data collector. All detections were made by using Doppler filtering. However, no positioning of the object was made. By being able to locate objects around the corner, not only moving objects could be detected, but an image could be produced for both detection and target classification.

In this paper we propose a positioning algorithm for out of line-of-sight radar applications. The algorithm is based on an *a priori* knowledge of the scene. A reference signal of the scene is computed using Geometrical Optics, GO, and a simplified diffraction term. The algorithm is tested on simulated data generated by using various methods like GO, Uniform Theory of Diffraction, UTD [5] and Physical Optics, PO. The positioning algorithm is demonstrated considering an array antenna solution.

2. Algorithm description

A simplified street corner scenario described in Fig. 1 is considered. We assume that the transmitter and receiver positions at T and R, relative to the origin O, and that the street width d, are known. In real situations these positions and distances could be found using a simple laser range finder.

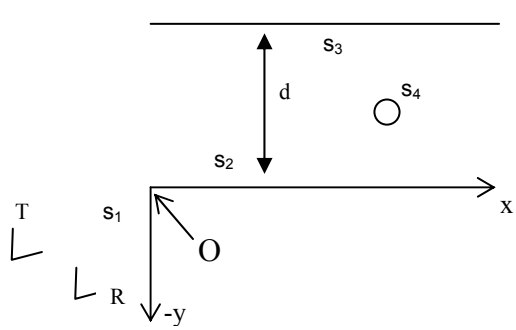

Fig. 1. *Overview of typical street corner where O is the origin of the coordinate system, S_1, S_2, S_3 are the boundaries of the vertical walls near the street corner and S_4 is the target location. The transmitting and receiving antennas are denoted T and R.*

978-1-4244-6051-9/11/$26.00 ©2011 IEEE

The main idea behind the algorithm is to estimate the scene transfer function and to use it when calculating a reference signal that is used in the imaging algorithm. To compute the transfer function a number of approximations are introduced as follows.

1. The scattered field is calculated using the GO-approximation, which means that the scattered field at every point is that of an infinite structure.
2. The boundaries S_1 ,S_2, and S_3 are considered to be smooth Perfect Electric Conductors (PEC).
3. Only a scalar problem is considered in the reference signal of Eq (2).
4. Diffraction at the origin, O, is written according to Eq (3).
5. The distance, d, between S_2 and S_3 is known and also the receiver and transmitter positions relative to the origin, O, are known.
6. The Born approximation is used, hence all scatterers are considered weak.

Consider a point scatterer located at $\boldsymbol{r_s}$. The approximations 1-6 implies that the received scalar field, $E_r(\boldsymbol{r_r}, \boldsymbol{r_t}, \boldsymbol{r_s}, k)$, at $\boldsymbol{r_r}$ can be written as:

$$E_r(\boldsymbol{r_r}, \boldsymbol{r_t}, \boldsymbol{r_s}, k) = G(\boldsymbol{r_r}, \boldsymbol{r_t}, \boldsymbol{r_s}, k) E_t(\boldsymbol{r_t}, k) \tag{1}$$

where $E_t(\boldsymbol{r_t}, k)$ is the transmitted field, k is the wavenumber and $G(\boldsymbol{r_r}, \boldsymbol{r_t}, \boldsymbol{r_s}, k)$ is the transfer function:

$$G(\boldsymbol{r_r}, \boldsymbol{r_t}, \boldsymbol{r_s}, k) = S_t S_r \{ \textstyle\sum_{m=1}^{n_b} g(k, |\boldsymbol{r_s} - \boldsymbol{r_{t,m}}|) g(k, |\boldsymbol{r_{r,m}} - \boldsymbol{r_s}|) \} + g_d(\boldsymbol{r_t}, \boldsymbol{r_s}, \boldsymbol{r_r}) \tag{2}$$

where n_b is the number of bounces taken into account. The term g_d is a simplified diffraction transfer function written according to Eq (3). The free space Green's function is given by g, S_t and S_r = 0 or 1, is the shadowing function, due to the corner, for the rays from the transmitter, and towards the receiver, respectively. The rest of the parameters are defined in Fig. 2.

$$g_d(\boldsymbol{r_t}, \boldsymbol{r_s}, \boldsymbol{r_r}) = \frac{e^{-ik(|\boldsymbol{r_t}| + 2|\boldsymbol{r_s}| + |\boldsymbol{r_r}|)}}{|\boldsymbol{r_t}||\boldsymbol{r_s}|^2|\boldsymbol{r_r}|} \tag{3}$$

The diffraction term g_d includes only the field contribution between transmitter-corner-object-corner-receiver.

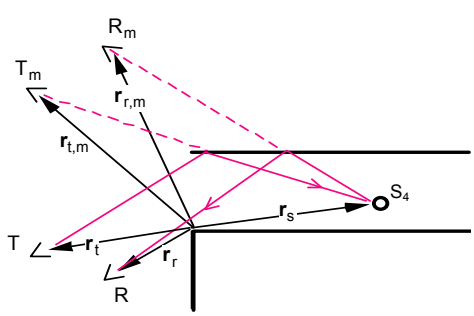

Fig. 2. *Parameter definitions. The multipath propagation between an antenna (T, R) and the scatterer at* $\boldsymbol{r_s}$ *via a wall reflection is equivalent, in GO, to free-space propagation between the antenna mirror point of the reflecting wall and the scatterer. The figure only shows the mirror positions for one bounce, m=1.*

3. Imaging algorithm

Consider a calculated or measured signal $M_{t,r}$ transmitted from transmitter *t* and received in receiver *r*, assumed to be $M_{t,r}(\boldsymbol{r_r}, \boldsymbol{r_t}, \boldsymbol{r_s}, k) \propto E_r(\boldsymbol{r_r}, \boldsymbol{r_t}, \boldsymbol{r_s}, k)$. Let $\boldsymbol{r_p}$ be a pixel in the image. We calculate the reference signal $E_r(\boldsymbol{r_r}, \boldsymbol{r_t}, \boldsymbol{r_p}, k)$ through Eq (1)-(3). It can be shown [6] that by transmitting a phase conjugate of the

received field the antenna will be focused on the scatterer present in the scene. We therefore define the imaging algorithm at pixel $\boldsymbol{r_p}$ as:

$$I(\boldsymbol{r_p}) = \sum_{r=1}^{n_r} M_r(\boldsymbol{r_{r,p}}) = \sum_{r=1}^{n_r}\sum_{i=1}^{n_k}\sum_{t=1}^{n_t} E_r(\boldsymbol{r_r}, \boldsymbol{r_t}, \boldsymbol{r_p}, k_i)\overline{M_{t,r}(\boldsymbol{r_r}, \boldsymbol{r_t}, \boldsymbol{r_s}, k_i)} \tag{4}$$

where n_r,n_k,n_t, are the number of receivers, transmitted frequencies and transmitters. The overbar denotes complex conjugation.

4. Results

The reference function given in Eq (2) does not give any height information; therefore we consider only 2-dimensional cases here. In the scenario all the walls are vertically placed, hence the mirror points will be in the same plane. To get height information one must either take into account ground interactions or use an antenna with a synthetic or large real aperture. First we demonstrate the effect of including the diffraction term g_d in Eq (3). In Fig. 3 we show simulated results from a point scatterer positioned at $\boldsymbol{r_s} = [4,\ 1\ ]$ m. $M_{t,r}$ is calculated using UTD and GO. Since the edge is a vertical structure and we want as strong diffracted field in the shadow region as possible we only consider polarisation orthogonal to the edge, H-polarisation. The simulated antenna is a 50 cm long 1-dimensional 34 element array, horizontally positioned parallel to the x-axis and centred at $\boldsymbol{r_t} = [-3.99,\ 4\ ]$ m. The antenna transmits and receives at each element, hence $\boldsymbol{r_t} = \boldsymbol{r_r}$. The bandwidth is 2 GHz centred at 10 GHz.

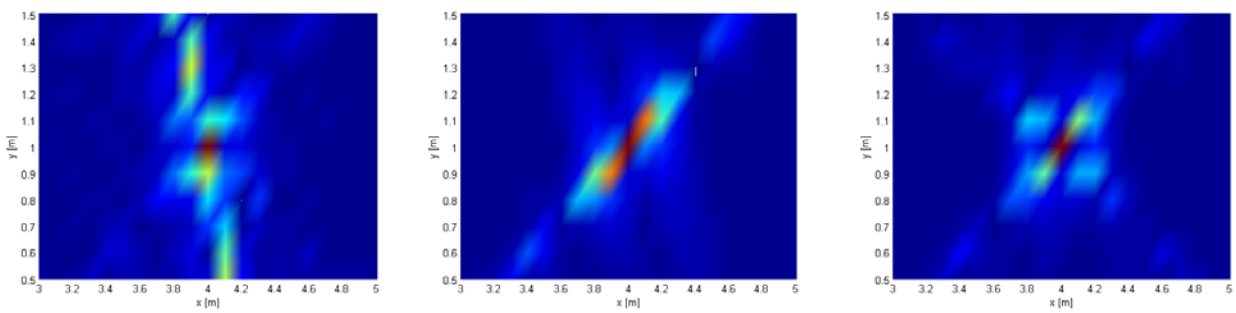

(a) (b) (c)

Fig. 3 (a)-(c). *Images of a point scatterer at* $\boldsymbol{r_s} = [4,\ 1]$ *m. The RCS of the object along* $\boldsymbol{r_s}$ *is chosen 40 dB higher than the RCS of the multiple bounces (*$\boldsymbol{r_{t,m}}$*). The scenario is given in Fig.1 with the street width d = 4 m. In (a) 4 bounces have been used in the reference signal. Figures (b) and (c) show the results with* g_d *omitted for 1 and 4 bounces respectively.*

In Fig. 3 (a) the diffraction term, g_d, has been amplified 40 dB just to show a possible effect. Usually the diffraction component is weak but for some objects, like a trihedral direct towards the corner, this component is not negligible. We see in Fig. 3 (a) that only by including one diffraction term, large sidelobes are created at a circle centered at the edge. However comparing with Fig. 3 (c), where g_d is omitted, the width of the mainlobe has slightly decreased. By including more bounces, the sidelobes are reduced and the resolution increases. For walls with low reflectivity the magnitude of the higher order bounces reduces, not only by the distance, but also due to absorption and transmission effects through the walls. To get better performance the received signal and the reference signal could be multiplied with a time growing function to account for such effects. By using an array antenna the sidelobes are reduced. The algorithm is sensitive to the assumption that the mean distance between the walls is constant. If this is not the case, the results will be defocused, to what degree depends on the deviation from the assumed distance, d.

The algorithm has been tested on a more realistic 3D-scenario shown in Fig. 4 (a). Here $M_{t,r}$ has been calculated using a commercial software, FERMAT. FERMAT uses shooting and bouncing ray technique [7] in combination with PO to compute the received signal. The antenna is the same as in previous calculations. The street is surrounded by 4 m high, 20 cm thick, dry concrete walls with $\epsilon_r = 6$ and $\sigma = 2$ mS/m. A CAD-model of a

human, made of 13400 polygons is positioned at $\boldsymbol{r_s} = [4,\ 1,\ 0]$ m. The street is considered to be made of infinitely thick concrete. All walls are smooth.

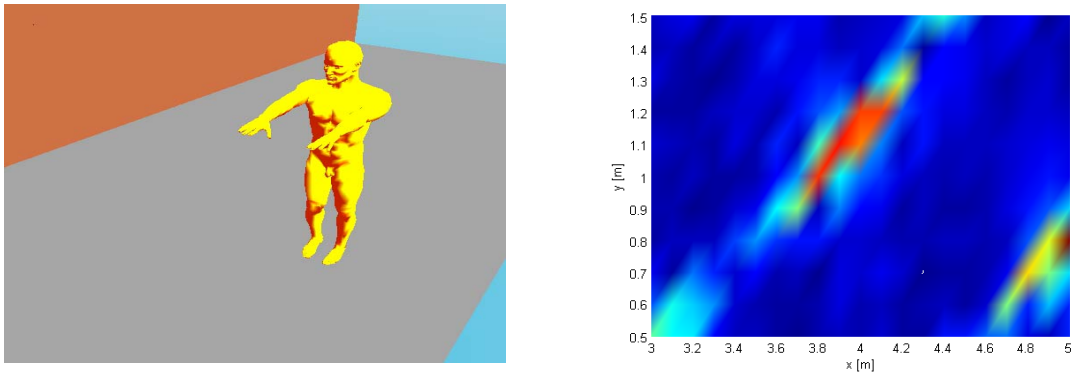

(a) (b)

Fig. 4 (a)-(b). *Scenario overview (a). Positioning results (b). The reference signal is calculated using 4 bounces and g_d is omitted. The bandwidth of the radar is 2 GHz and HH-polarisation is considered.*

We see that the position of the human is detected by the algorithm, but there is also a "ghost" detection at x = 5 m, y = 0.7 m. This detection is actually the strongest and corresponds to an interaction not taken into account in the reference signal. However the resolution is too poor in this case to see that there actually is a human. By using a larger bandwidth along with a vertical scan, 3D-images can be produced in which a human might be detected. For moving targets, zero-doppler filtering can be made to filter out stationary clutter.

5. Conclusions

We have demonstrated a positioning algorithm for see-around corner applications with radar. The algorithm is based on *a priori* knowledge about the scene and Geometrical Optics to calculate a reference signal, used to produce the pixel intensities in an image of the scenery, by correlation with the backpropagated received field at the target scatterer position. Work in progress is to include a more advanced reference signal which will reduce "ghost positions".

6. References

1. A. Sume, M. Gustafsson, A. Jänis, S. Nilsson and A. Örbom, "See-around-corners with coherent radar," presented at 20th Nordic Conference on Radio Science and Communication, RVK 2008, Växjö, Sweden, 2008.

2. A. Sume, M. Gustafsson, A. Jänis, S. Nilsson, J. Rahm and A. Örbom, "Radar detection of moving objects around corners," presented at SPIE Radar Sensor Technology XIII, 2009.

3. A. Sume, S. Nilsson, J. Rahm and A. Örbom, "Radar measurements with realistic wall type for verification of the see-around-corners principle," Swedish Defence Research Agency, Linköping, Sweden, Technical report FOI-R--2688--SE, 2007 (in Swedish).

4. A. Sume, M. Gustavsson, M. Herberthson, A. Jänis, S. Nilsson, J. Rahm, A. Örbom, "Radar Detection of moving targets behind corners," *IEEE Transactions on Geoscience and Remote Sensing*, 2011 (in press).

5. D. A. McNamara, C. W. I. Pistorius, and J. A. G. Malherbe, *Introduction to the Uniform Theory of Diffraction*. Norwood MA: Artech House, 1990.

6. M. I. Skolnik and D. D. King, "Self phasing array antennas," *IEEE Transactions on Antennas and Propagation*, vol. AP-12, pp. 142-149, 1964.

7. H. Ling, R.-C. Chou, and S.-W. Lee, "Shooting and Bouncing Rays: Calculating the RCS of an Arbitrary Shaped Cavity," *IEEE Transactions on Antennas and Propagation*, vol. 37, pp. 194-204, 1989.